ARTICLE

# Antileukemic activity and mechanism of action of the novel PI3K and histone deacetylase dual inhibitor CUDC-907 in acute myeloid leukemia

**Xinyu Li,[1#] Yongwei Su,[1#] Gerard Madlambayan,[2] Holly Edwards,[3,4] Lisa Polin,[3,4] Juiwanna Kushner,[3,4] Sijana H. Dzinic,[3,4] Kathryn White,[3,4] Jun Ma,[1] Tristan Knight,[5,6] Guan Wang,[1] Yue Wang,[7] Jay Yang,[3] Jeffrey W. Taub,[5,6] Hai Lin,[8] and Yubin Ge[3,4,6]**

[1]National Engineering Laboratory for AIDS Vaccine, Key Laboratory for Molecular Enzymology and Engineering, the Ministry of Education, School of Life Sciences, Jilin University, Changchun, P.R. China; [2]Department of Biological Sciences, Oakland University, Rochester, MI, USA; [3]Department of Oncology, Wayne State University School of Medicine, Detroit, MI, USA; [4]Molecular Therapeutics Program, Barbara Ann Karmanos Cancer Institute, Wayne State University School of Medicine, Detroit, MI, USA; [5]Division of Pediatric Hematology/Oncology, Children's Hospital of Michigan, Detroit, MI, USA; [6]Department of Pediatrics, Wayne State University School of Medicine, Detroit, MI, USA; [7]Department of Pediatric Hematology and Oncology, The First Hospital of Jilin University, Changchun, P.R. China and [8]Department of Hematology and Oncology, The First Hospital of Jilin University, Changchun, P.R. China

*[#]XL and YS contributed equally to this work.*

Ferrata Storti Foundation

**Haematologica** 2019
Volume 104(11):2225-2240

## ABSTRACT

Induction therapy for patients with acute myeloid leukemia (AML) has remained largely unchanged for over 40 years, while overall survival rates remain unacceptably low, highlighting the need for new therapies. The PI3K/Akt pathway is constitutively active in the majority of patients with AML. Given that histone deacetylase inhibitors have been shown to synergize with PI3K inhibitors in preclinical AML models, we investigated the novel dual-acting PI3K and histone deacetylase inhibitor CUDC-907 in AML cells both *in vitro* and *in vivo*. We demonstrated that CUDC-907 induces apoptosis in AML cell lines and primary AML samples and shows *in vivo* efficacy in an AML cell line-derived xenograft mouse model. CUDC-907-induced apoptosis was partially dependent on Mcl-1, Bim, and c-Myc. CUDC-907 induced DNA damage in AML cells while sparing normal hematopoietic cells. Downregulation of CHK1, Wee1, and RRM1, and induction of DNA damage also contributed to CUDC-907-induced apoptosis of AML cells. In addition, CUDC-907 treatment decreased leukemia progenitor cells in primary AML samples *ex vivo*, while also sparing normal hematopoietic progenitor cells. These findings support the clinical development of CUDC-907 for the treatment of AML.

## Introduction

Acute myeloid leukemia (AML) is a myeloid malignancy characterized by increased self-renewal, limited differentiation, and deregulated proliferation of myeloid blasts.[1] Little has changed in the treatment of AML over the past 40 years. Despite low overall 5-year survival rates (~25% for adults and ~65% for children)[2], standard induction therapy for AML patients continues to consist of cytarabine and an anthracycline (e.g., daunorubicin) backbone. The major contributor to such low overall survival rates is resistance to chemotherapy. Leukemia-initiating cells are one population thought to be responsible for relapse. Due to the quiescent nature of leukemia-initiating cells, current chemotherapy is often incapable of fully eradicating all these cells.[3] Therefore, new therapies that not only eliminate bulk leukemia cells but also eradicate leukemia-initiating cells are urgently needed to improve the overall survival rates of people with this deadly disease.

**Correspondence:**

*YUBIN GE*
gey@karmanos.org

*HAI LIN*
maillinhai@sina.com

Received: July 5, 2018.

Accepted: February 28, 2019.

Pre-published: February 28, 2019.

doi:10.3324/haematol.2018.201343

*Check the online version for the most updated information on this article, online supplements, and information on authorship & disclosures: www.haematologica.org/content/104/11/2225*

The phosphoinositide 3-kinase (PI3K)/mammalian target of rapamycin (mTOR) pathway is involved in cellular proliferation, differentiation, and survival. It has been reported that 50-80% of AML patients have a constitutively active PI3K/mTOR pathway, which correlates with very poor prognosis.[4,5] In addition, aberrant activation of the PI3K pathway is a feature of leukemia-initiating cells.[6,7] Although PI3K inhibitors have been shown to target AML cells, including leukemia-initiating cells, clinical results have been disappointing, likely due to compensatory activation of other survival pathways.[8-10] Thus, PI3K inhibitors must be used in combination to prevent compensation by other survival pathways and ensure successful eradication of AML cells.

Preclinical testing has revealed promising anti-cancer activity for the combination of PI3K inhibitors with histone deacetylase (HDAC) inhibitors.[11-13] This prompted the design and synthesis of the dual PI3K and HDAC inhibitor CUDC-907 (fimepinostat).[14] CUDC-907 has shown encouraging preclinical activity against multiple types of cancers and the drug is currently being tested in phase I and II clinical trials for the treatment of lymphoma, multiple myeloma, and advanced/relapsed solid tumors (*www.clinicaltrials.gov*).[15-17] It has shown such promising clinical efficacy that the US Food and Drug Administration recently granted Fast Track designation to CUDC-907 for the treatment of adults with relapsed or refractory diffuse large B-cell lymphoma (*http://www.curis.com/*). In this study, we investigated CUDC-907 in AML cell lines, primary AML samples, and a cell line-derived xenograft AML model. We showed that CUDC-907 induces apoptosis in AML cell lines and primary AML samples and this effect is, at least partially, mediated by Mcl-1, Bim, and c-Myc. Additionally, CUDC-907 treatment down-regulates CHK1, Wee1, and ribonucleotide reductase (RR) catalytic subunit M1 (RRM1) and induces DNA replication stress and damage. *In vivo* results show that CUDC-907 has potential for the treatment of AML.

## Methods

A detailed description of the methods is given in the *Online Supplementary Material*.

### Cell culture

The characteristics of the cell lines are presented in *Online Supplementary Table S1*.

### Clinical samples

Diagnostic AML blast samples were obtained from patients at the First Hospital of Jilin University (Changchun, China). Written informed consent was provided according to the Declaration of Helsinki. The Human Ethics Committee of the First Hospital of Jilin University approved this study. Clinical samples were screened for gene mutations by polymerase chain reaction (PCR) amplification and automated DNA sequencing, and fusion genes by real-time reverse transcriptase PCR, as described previously.[18,19] The patients' characteristics are presented in *Online Supplementary Table S2*. Samples were chosen based on availability of adequate material at the time the assay was performed.

### Annexin V/propidium iodide staining

Apoptosis was determined using an Annexin V-Fluorescein Isothiocyanate (FITC)/Propidium Iodide (PI) Apoptosis Kit (Beckman Coulter; Brea, CA, USA), as described elsewhere.[20,21] The mean percentage (± standard error of mean) of annexin$V^+/PI^-$ (early apoptotic) and annexin $V^+/PI^+$ (late apoptotic and/or dead) cells from one representative experiment is shown.

### Colony formation assay

Cells were treated with CUDC-907 for 24 h, washed with phosphate-buffered saline, plated in triplicate in MethoCult (Stem Cell Technologies, Cambridge, MA, USA) and incubated for 10-14 days, according to the manufacturer's instructions. Colony-forming units were visualized using an inverted microscope and colonies containing >50 cells were enumerated.

### Leukemia xenograft model

Immunocompromised triple transgenic NSG-SGM3 female mice at 8 weeks of age [NSGS, JAX#103062; non-obese diabetic scid gamma (NOD.Cg-Prkdc$^{scid}$ Il2rg$^{tm1Wjl}$ Tg(CMV-IL3, CSF2, KITLG)1Eav/MloySzJ; Jackson Laboratory, Bar Harbor ME, USA] were injected with MV4-11 cells (1 x $10^6$ cells/mouse; 0.2 mL/injection) intravenously (day 0). Mice were randomly divided into three groups (5 mice/group; day 3): one group was the no treatment control group, the other two groups were given 100 or 150 mg/kg CUDC-907 [3% ethanol (200 proof), 1% Tween-80 (polyoxyethylene 20 sorbitan monooleate) and sterile water; all USP grade; v/v)]. Mice were treated daily for 8 days followed by 4 days off treatment, and then treated for a further 6 days. Body weights were recorded daily and condition assessed (at least twice daily) for the duration of the study. Mice were humanely euthanized when they presented with: >20% weight loss, decreased mobility limiting access to food and water, lymph node metastases, progressive anemia, or lateral recumbency. The percentage increase in lifespan (%ILS) was calculated: % ILS = [T-C/C] x 100 where "T" is the median day of death of treated mice and "C" is the median day of death of control animals. *In vivo* experiments were approved by the Institutional Animal Care and Use Committee at Wayne State University.

For the pharmacodynamics study, NSG mice were injected with MV4-11 cells (1 x $10^7$ cells/mouse) intravenously. Twenty-one days later, mice were randomized (5 mice/group) and injected once with vehicle control, 100 or 150 mg/kg CUDC-907. The mice were sacrificed 24 h later and bone marrow cells were collected. Human cells were enriched using the EasySep Mouse/Human Chimera Isolation Kit (Stem Cell Technologies).

### Statistical analysis

Differences were compared using the pair-wise two-sample *t*-test (comparisons of apoptosis, colony-forming units, and %DNA in the tail) or the Mann-Whitney two-sample U test [comparison of CUDC-907 half maximal inhibitory concentration ($IC_{50}$)]. The overall survival probability was estimated using the Kaplan-Meier method and the statistical analysis was performed using the log-rank test. The statistical computations were conducted using GraphPad Prism 5.0. The level of statistical significance was set at $P<0.05$.

## Results

### CUDC-907 decreases viable cells and induces apoptosis in acute myeloid leukemia cell lines, and shows promise against a MV4-11-derived xenograft model *in vivo*

CUDC-907 $IC_{50}$ for seven AML cell lines, as measured by MTT assays, ranged from 12.4 nM (for MOLM-13) to 73.7 nM (for CTS) (Figure 1A). Annexin V/PI staining and flow cytometry analysis revealed that treatment with

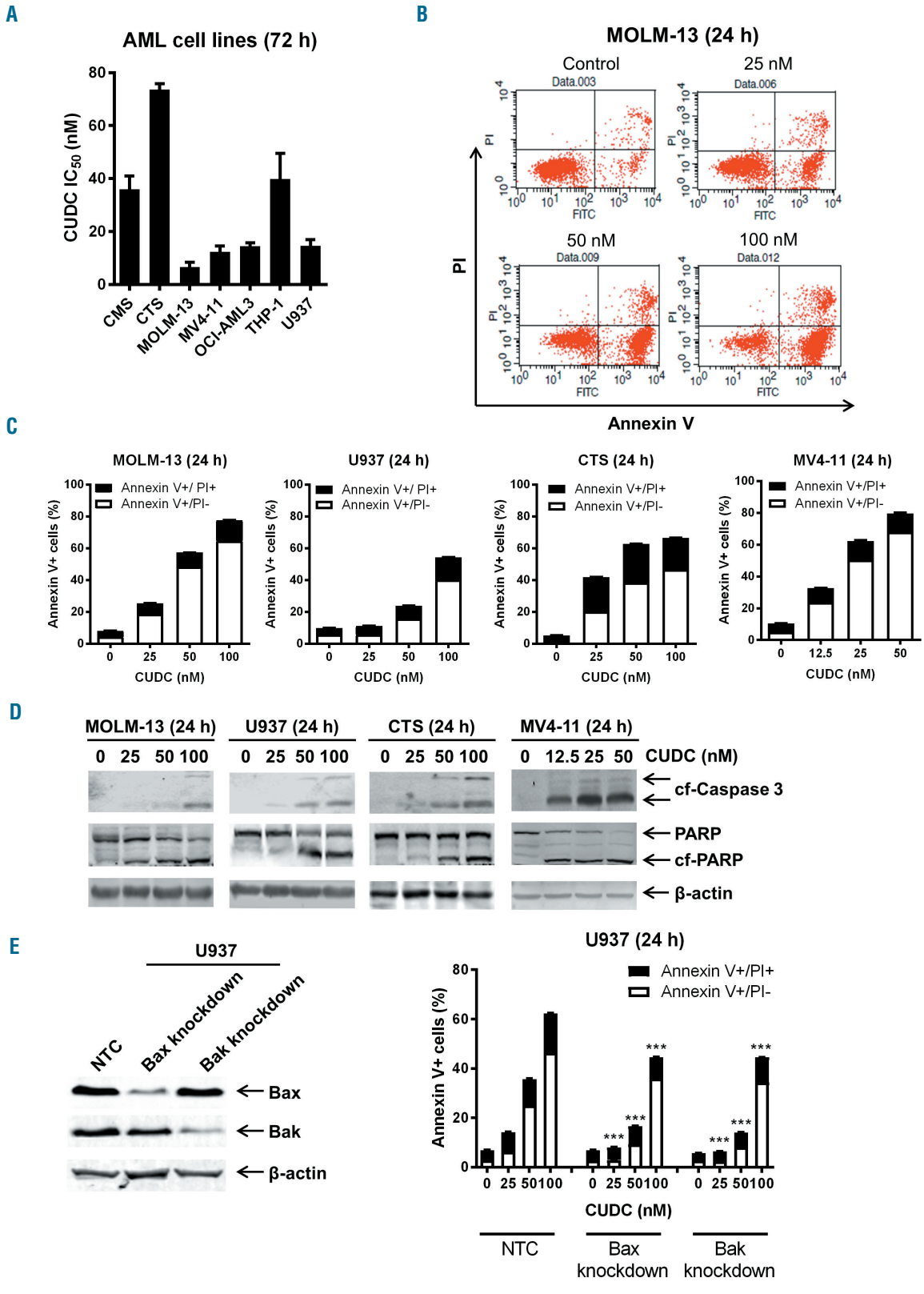


**Figure 1. CUDC-907 treatment decreases viable cells and induces apoptosis in acute myeloid leukemia cell lines and shows promise in an acute myeloid leukemia cell line-derived mouse model.** (A) Acute myeloid leukemia cell lines were treated with variable concentrations of CUDC-907 for 72 h and viable cells were determined using MTT reagent. Data are shown as mean ± standard error of mean (SEM). (B, C) MOLM-13, U937, CTS, and MV4-11 cells were treated with CUDC-907 for 24 h and then subjected to annexin V-FITC/propidium iodine (PI) staining and flow cytometry analyses. Representative dot plots are shown in panel (B). Mean percent annexin V$^+$ cells ± SEM are shown in panel (C). (D) MOLM-13, U937, CTS, and MV4-11 cells were treated with CUDC-907 for 24 h. Whole cell lysates were subjected to western blotting. (E) U937 cells were infected with NTC-, Bax-, or Bak-shRNA lentivirus particles overnight, then washed and incubated for 48 h prior to the addition of puromycin to the culture medium. Whole cell lysates of puromycin-resistant cells were subjected to western blotting (left panel). U937 NTC, Bax knockdown, and Bak knockdown cells were treated with CUDC-907 for 24 h and then subjected to annexin V/PI staining and flow cytometry analysis (right panel). ***$P$<0.001. (continued on the next page).

CUDC-907 for 24 h caused an increase in annexin V$^+$ cells, which was accompanied by increased cleaved caspase 3 and PARP (Figure 1B-D), demonstrating that the cells underwent apoptosis. Short hairpin (sh)RNA knockdown of Bax and Bak partially rescued U937 cells from CUDC-907-induced apoptosis (Figure 1E). Furthermore, overexpression of Bcl-xL abolished CUDC-907-induced apoptosis demonstrating that CUDC-907 induces apoptosis through the intrinsic apoptosis pathway (Figure 1F). The potential *in vivo* efficacy of CUDC-907 was evaluated in an early stage MV4-11-derived xenograft mouse model. Mice were treated with CUDC-907 daily for 8 days, given 4 days off treatment, and then treated daily for another 6 days (Figure 1G). All mice were given a 4-day break due to the 3% body weight loss in the mice treated with 150 mg/kg CUDC-907 after the initial eight doses (Figure 1H). This body weight loss was completely reversible within 4 days. The median survival following CUDC-907 treatment was 44 days for the animals given the 100 mg/kg dose and 47 days for those given the 150 mg/kg, which are 11 and 14 days longer (or 33.3% and 42.2% increases in lifespan), respectively, than the median survival of the mice given the vehicle control (33 days; $P$=0.002) (Figure 1I). These results suggest that CUDC-907 treatment possesses modest antileukemic activity *in vivo*.

## CUDC-907 treatment decreases viable cells and induces apoptosis in primary acute myeloid leukemia samples from patients

CUDC-907 $IC_{50}$ ranged from 8.1 to 1,831 nM (*Online Supplementary Table S2*) in primary AML patient samples. Interestingly, samples from patients positive for *FLT3*-

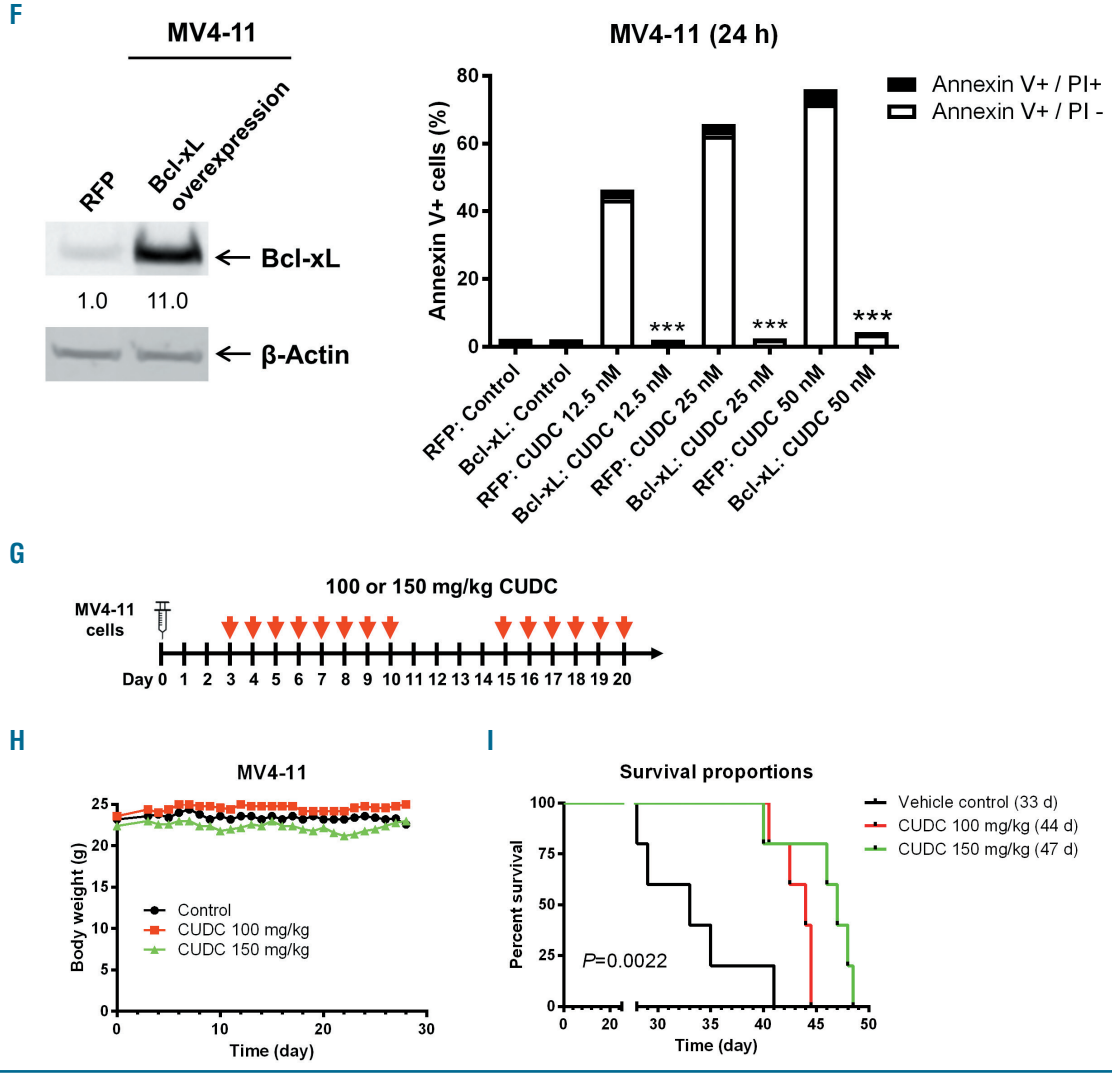


**Figure 1. Figure 1. CUDC-907 treatment decreases viable cells and induces apoptosis in acute myeloid leukemia cell lines and shows promise in an acute myeloid leukemia cell line-derived mouse model.** (continued from the previous page) (F) MV4-11 cells were infected with Precision LentiORF Bcl-xL and RFP control overexpression lentivirus particles overnight, then washed and incubated for 48 h prior to addition of blasticidin to the culture medium. Whole cell lysates were subjected to western blotting. The fold changes for the Bcl-xL densitometry measurements, normalized to β-actin and then compared to no drug treatment control, are indicated (left panel). The cells were treated with CUDC-907 for 24 h and then subjected to annexin V/PI staining and flow cytometry analysis. ***$P$<0.001 (right panel). (G-I) MV4-11 cells (1 x $10^6$ cells/mouse) were injected through the tail vein of immunocompromised NSGS mice. Three days after cell injection the mice were randomized (5 mice/group) and treated with vehicle control (3% 200 proof ethanol, 1% polyoxyethylene 20 sorbitan monooleate, and USP water), 100 mg/kg CUDC-907, or 150 mg/kg CUDC-907 for 8 consecutive days followed by 4 days off treatment, and then an additional 6 days of treatment. (H) Body weights were measured on a daily basis and are shown as mean ± SEM. (I) Overall survival probability, estimated with the Kaplan-Meier method. AML: acute myeloid leukemia; CUDC: CUDC-907; NTC: non-treated control; RFP: red fluorescent protein; cf-Caspase 3: cleaved caspase 3; cf-PARP: cleaved PARP.

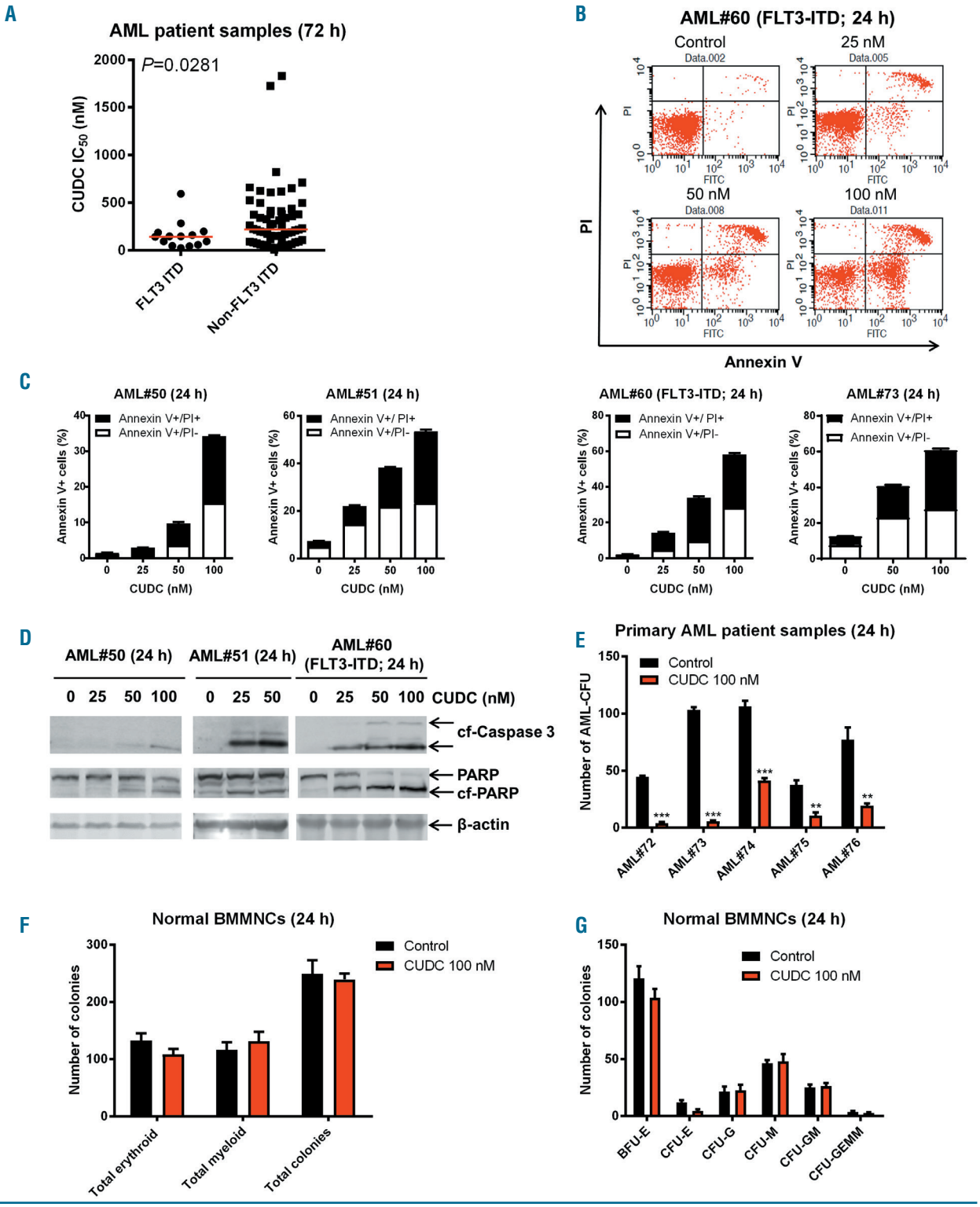


**Figure 2. CUDC-907 treatment induces apoptosis and inhibits colony formation in primary acute myeloid leukemia cells, but spares normal human bone marrow mononuclear cells.** (A) Primary samples from patients with *FLT3*-ITD-positive and *FLT3*-ITD-negative acute myeloid leukemia (AML) (n=14 and n=61, respectively) were treated with variable concentrations of CUDC-907 in 96-well plates for 72 h and then viable cells were determined using MTT reagent. The $IC_{50}$ values are means of duplicates from one experiment due to limited samples. The horizontal lines indicate the median. (B, C) Primary AML patient samples were treated with CUDC-907 for 24 h and then subjected to annexin V-FITC/propidium iodide (PI) staining and flow cytometry analyses. Representative dot plots are shown (B). Mean percent of annexin $V^+$ cells ± standard error of mean (SEM) are shown (panel C). (D) Primary AML patient samples were treated with CUDC-907 for 24 h. Whole cell lysates were subjected to western blotting. (E) Primary AML patient samples were cultured with vehicle control or 100 nM CUDC-907 for 24 h and then plated in methylcellulose. After incubation for 2 weeks, the number of surviving AML cells capable of generating leukemia colonies (AML-CFU) were enumerated. Data are presented as mean ± SEM. $^{**}P<0.01$, $^{***}P<0.001$. (F) Normal human bone marrow mononuclear cells from a single donor were cultured with vehicle control or 100 nM CUDC-907 for 24 h and then plated in methylcellulose. After incubation for 2 weeks, the number of surviving hematopoietic cells capable of generating colonies was counted. Total erythroid and myeloid colonies are presented as mean ± SEM. (G) The numbers of BFU-E, CFU-E, CFU-G, CFU-M, CFU-GM, and CFU-GEMM colonies are presented as mean ± SEM. AML: acute myeloid leukemia; CUDC: CUDC-907; cf-Caspase 3: cleaved caspase 3; cf-PARP: cleaved PARP; BMMNC: bone marrow mononuclear cells; BFU-E: burst-forming unit – erythroid; CFU-E: colony-forming unit - erythroid, CFU-G: colony-forming unit – granulocyte; CFU-M: colony-forming unit - monocyte, CFU-GM: colony-forming unit – granulocyte, macrophage; CFU-GEMM: colony-forming unit – granulocyte, erythroid, macrophage megaryocyte.

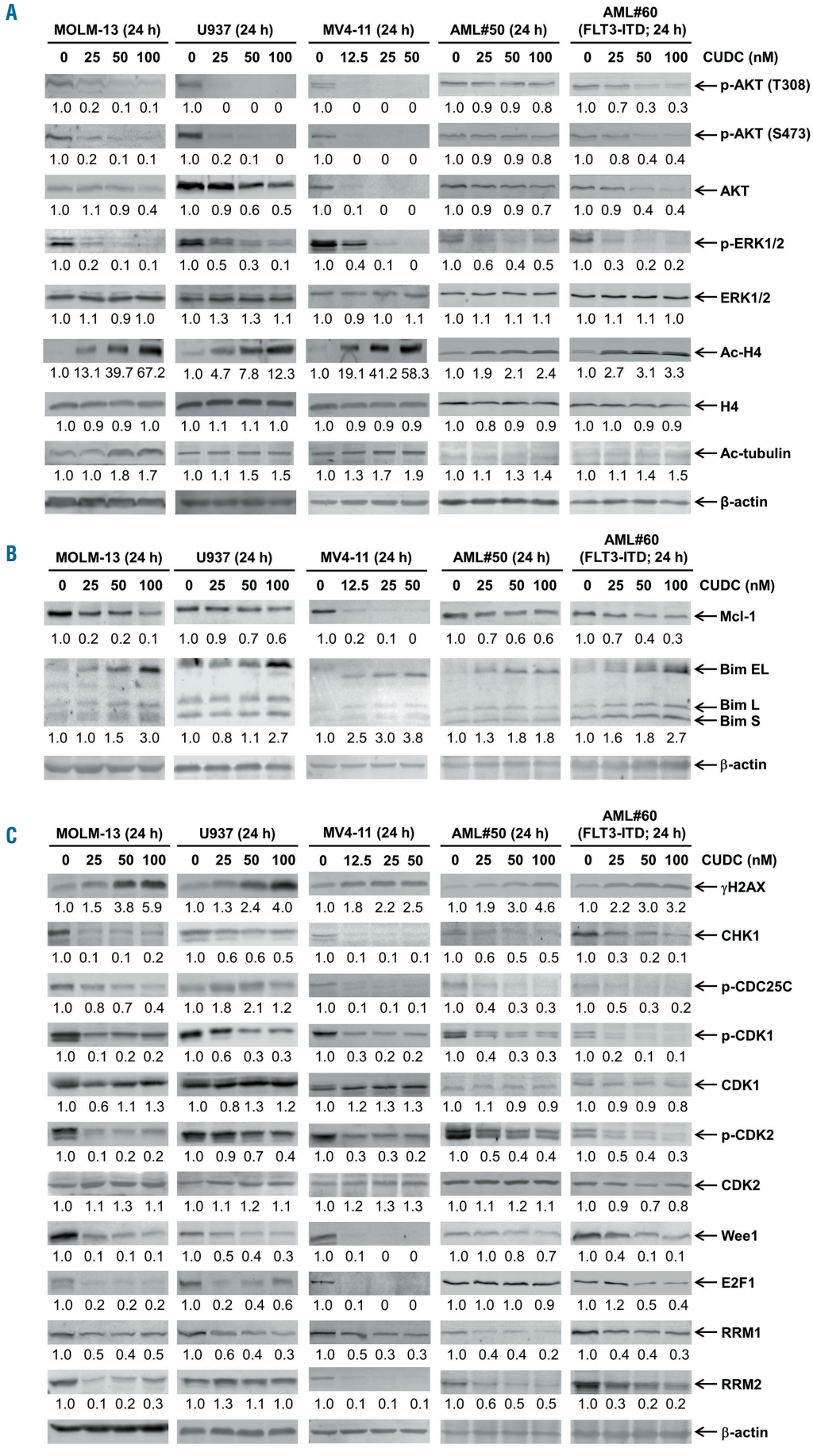


**Figure 3. CUDC-907 treatment inactivates PI3K and ERK and causes downregulation of Mcl-1, CHK1, Wee1, and RRM1, and upregulation of Bim and γH2AX.** (A-C) Acute myeloid leukemia (AML) cell lines and primary AML samples were treated with CUDC-907 for 24 h. Whole cell lysates were subjected to western blotting. The fold changes for the densitometry measurements, normalized to β-actin and then compared to no drug control, are indicated below the corresponding blot. Bim S, L, and EL indicate Bim short, long, and extra-long isoforms, respectively. (continued on the next page).

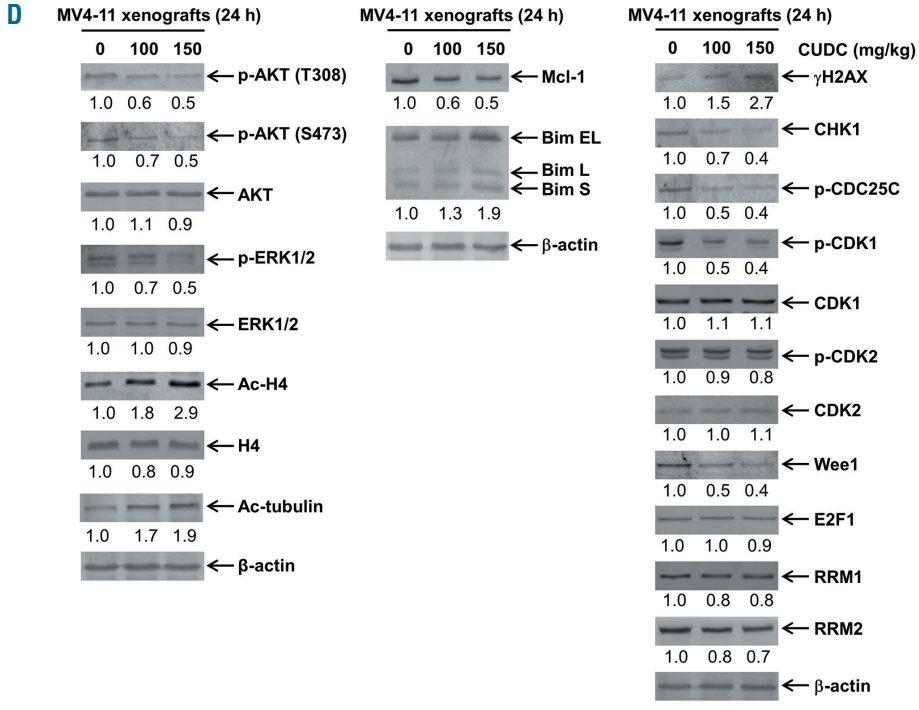


**Figure 3. CUDC-907 treatment inactivates PI3K and ERK and causes downregulation of Mcl-1, CHK1, Wee1, and RRM1, and upregulation of Bim and γH2AX.** (continued from the previous page) (D) NSG mice were injected with MV4-11 cells (1x10$^7$ cells/mouse). After 21 days, the mice were randomized into three groups and treated with the vehicle control or a single dose of CUDC-907. 24 h after treatment, the mice were sacrificed and bone marrow cells were harvested. Human cells were enriched as described in the Methods section. Whole cell lysates were subjected to western blotting. Normalized densitometry measurements are shown below the corresponding blot. CUDC: CUDC-907.

internal tandem duplication (ITD) (n=14, median $IC_{50}$ 143.3 nM) were significantly more sensitive to CUDC-907 than those from patients without *FLT3*-ITD (n=61, median $IC_{50}$ 217.6 nM; *P*=0.0281) (Figure 2A). CUDC-907 treatment induced a concentration-dependent increase of annexin V$^+$ cells accompanied by increased cleaved caspase 3 and PARP (Figure 2B-D), demonstrating that CUDC-907 treatment induced apoptosis in primary AML samples *ex vivo*. Next, we treated five primary AML samples with or without 100 nM CUDC-907 for 24 h and then plated the cells in methylcellulose. After 2 weeks, the number of surviving AML cells capable of generating leukemia colonies (AML-CFU) were enumerated. CUDC-907 treatment significantly reduced the number of AML-CFU in all samples tested, indicating that CUDC-907 treatment decreased leukemia progenitor cells (Figure 2E). In contrast, CUDC-907 treatment did not have a significant effect on colony formation of normal bone marrow mononuclear cells (Figure 2F, G), suggesting that CUDC-907 treatment spares normal hematopoietic progenitor cells.

## CUDC-907 downregulates Mcl-1, CHK1, Wee1, and RRM1, and upregulates Bim in acute myeloid leukemia cells

As previously reported,[15] CUDC-907 treatment decreased the levels of p-AKT (both T308 and S473) in three AML cell lines and two primary AML samples (Figure 3A). CUDC-907 treatment also decreased p-ERK1/2 levels, while total ERK levels remained relatively unchanged. p-AKT changes were detected as early as 3 h after CUDC-907 treatment in the cell lines (*Online Supplementary Figure S1*). These results confirm that CUDC-907 inactivated the PI3K/AKT and MEK/ERK pathways at these concentrations. Total AKT levels were decreased after 24 h of CUDC-907 treatment, although 3 h of treatment caused a decrease of p-AKT in the absence of changes in total AKT (*Online Supplementary Figure S1*). Increased acetylation of histone H4 and tubulin (deacetylated by HDAC6) was detected in the AML cell lines, confirming inhibition of HDAC at these concentrations as early as 3 h after treatment (Figure 3A and *Online Supplementary Figure S1*). Substantially increased acetylation of histone H4 was also detected in both primary AML samples, while the acetylation of tubulin was increased to a much lesser extent. Inhibition of the PI3K pathway and HDAC have been shown to cause downregulation of Mcl-1 and upregulation of Bim, respectively.[22-25] Accordingly, CUDC-907 treatment caused a reduction of Mcl-1 and an increase of Bim (Figure 3B), while Bcl-2, Bcl-xL, Bax, and Bak protein levels remained unchanged (*Online Supplementary Figure S2*). Based on the reports that HDAC inhibitors can downregulate DNA damage response proteins,[23-26] we looked at γH2AX (a potential biomarker of DNA double-strand breaks), DNA damage response proteins CHK1, Wee1, and related downstream proteins. CUDC-907 treatment caused an increase of γH2AX and decreases of CHK1, p-CDK1, p-CDK2, Wee1, and RRM1 in AML cell lines and primary AML samples (Figure 3C). Total CDK1 and CDK2 levels were largely unaffected. p-CDC25C and RRM2 decreased, except in U937 cells. E2F1 levels decreased in the cell lines and in one primary AML samples. These results suggest that CUDC-907 may induce DNA damage, which causes death of AML cells. The above results were further confirmed in the MV4-11 xenograft mouse model following administration of a single dose of CUDC-907 (Figure 3D). Downregulation of CHK1, Wee1, and RRM1 by CUDC-907 treatment was not affected by the pan-caspase inhibitor Z-VAD-FMK (*Online Supplementary Figure S3*). In contrast, Z-VAD-FMK treatment itself caused an increase in Mcl-1 protein levels, suggesting that caspases are involved in the regulation of Mcl-1 protein. Surprisingly, co-treatment of AML cells with CUDC-907 and Z-VAD-FMK resulted in substantial-

ly increased Mcl-1 protein levels compared to Z-VAD-FMK alone (*Online Supplementary Figure S3*). Using the parental compounds of CUDC-907, SAHA (a pan-HDAC inhibitor) and GDC-0941 (a PI3K inhibitor), alone or combined (at a 1:1 ratio) at inhibitory concentrations, we found that SAHA and GDC-0941 synergistically induced apoptosis (*Online Supplementary Figure S4A, C*). The half maximal effective concentrations ($EC_{50}$) were much higher for the combination of SAHA plus GDC-0941 than for CUDC-907, suggesting that while they do synergize, the hybrid is more potent than the parental compounds.

Western blotting analysis of whole cell lysates from MOLM-13 cells treated with CUDC-907 for up to 24 h, revealed decreased Mcl-1 and increased Bim, cleaved caspase 3, and cleaved PARP at the 12 h time-point (Figure 4A). Decreased RRM1 and CHK1, and increased γH2AX were also detected at the 12 h time-point, while decreased Wee1 was detected as early as 4 h after CUDC-907 treatment (Figure 4B). Similar protein level changes were detected 16 h after treatment in U937 cells (*Online Supplementary Figure S5*). Annexin V/PI staining revealed a significant increase in annexin $V^+$ cells, indicating that

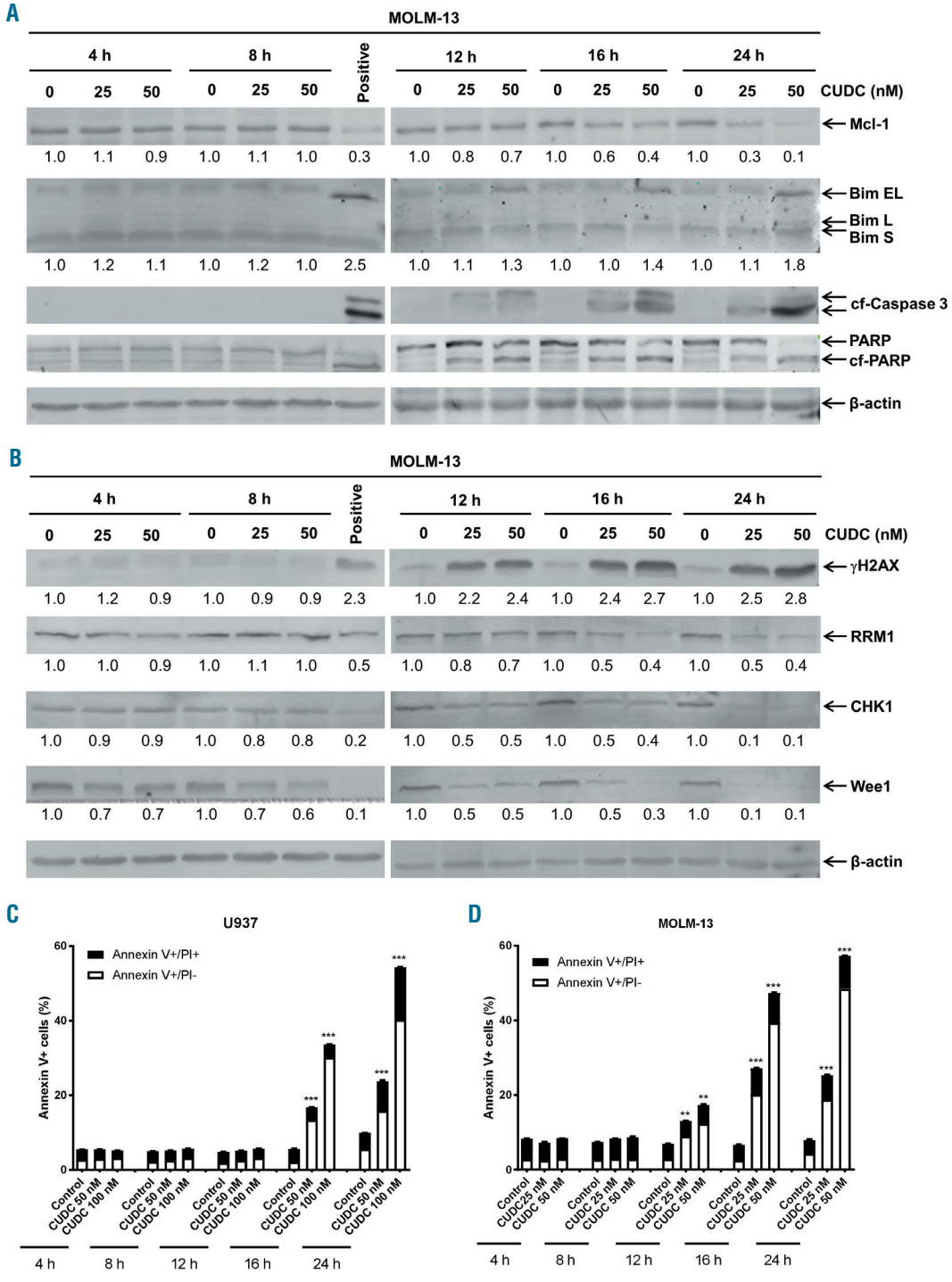


**Figure 4. Upregulation of Bim and downregulation of Mcl-1, CHK1, Wee1, and RRM1 coincide with induction of apoptosis.** (A, B) MOLM-13 cells were treated with CUDC-907 for up to 24 h. Whole cell lysates were subjected to western blotting and probed with the indicated antibodies. The fold changes for the densitometry measurements, normalized to β-actin and then compared to no drug control, are indicated below the corresponding blot. Cells treated with 50 nM CUDC-907 for 24 h were used as a positive control for γH2AX and cleaved caspase 3. (C, D) U937 (C) and MOLM-13 (D) cells were treated with CUDC-907 for up to 24 h and then subjected to annexin V-FITC/propidium iodide (PI) staining and flow cytometry analyses. Mean percent annexin $V^+$ cells ± standard error of mean are shown. $^{**}P<0.01$, $^{***}P<0.001$. Bim S, L, and EL indicate Bim short, long, and extra-long isoforms, respectively. CUDC: CUDC-907; cf-Caspase 3: cleaved caspase 3; cf-PARP: cleaved PARP.

induction of apoptosis begins at 12 h for MOLM-13 cells and 16 h for U937 cells (Figure 4C, D). Taken together, these results suggest that these changes in protein levels coincide with the induction of apoptosis.

### Mcl-1 and Bim play important roles in CUDC-907-induced apoptosis

To confirm the roles of Mcl-1 and Bim in CUDC-907-induced apoptosis, Mcl-1 overexpression and Bim shRNA knockdown were performed in U937 cells. Western blot analysis confirmed overexpression of Mcl-1 and knockdown of Bim (Figure 5A, B; left panels). Annexin V/PI staining and flow cytometry analysis revealed that Mcl-1 overexpression and Bim knockdown partially prevented CUDC-907-induced apoptosis (Figure 5A, B; right panels), providing evidence that Mcl-1 and Bim play roles in CUDC-907-induced apoptosis. Real-time reverse transcriptase PCR results showed that CUDC-907 treatment caused a concentration-dependent and significant increase of Bim transcripts, while Mcl-1 transcript levels remained largely unchanged in both AML cell lines and two primary patient samples (Figure 5C, D). Similar results were

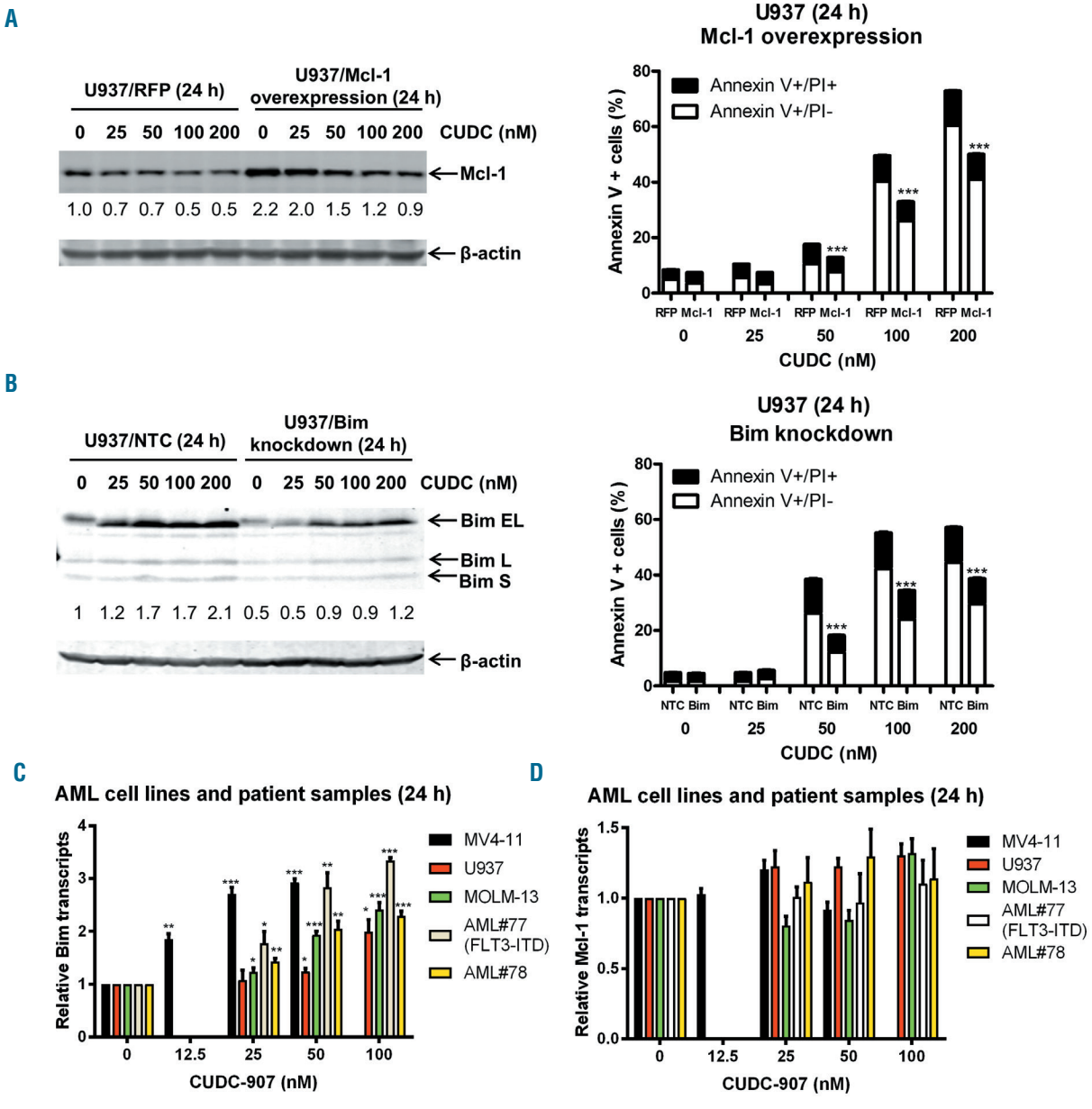


**Figure 5. Mcl-1 and Bim play important roles in CUDC-907-induced apoptosis in acute myeloid leukemia cells.** (A, B) U937 cells were infected with Precision LentiORF Mcl-1 (U937/Mcl-1) and RFP control (U937/RFP) (A) or NTC- (U937/NTC) and Bim-shRNA (U937/Bim) (B) lentivirus particles overnight, then washed and incubated for 48 h prior to the addition of blasticidin or puromycin, respectively, to the culture medium. The antibiotic-resistant cells were treated with CUDC-907 for 24 h. Whole cell lysates were subjected to western blotting. The fold changes for the Mcl-1 or Bim densitometry measurements, normalized to β-actin and then compared to no drug treatment control, are indicated (left panel). The cells were treated with CUDC-907 for 24 h and then subjected to annexin V/propidium iodide staining and flow cytometry analysis. ***$P$<0.001 (right panel). Bim S, L, and EL indicate Bim short, long, and extra-long isoforms, respectively. (C, D) MV4-11, U937 and MOLM-13 AML cell lines and two primary AML patient samples were treated with 0-100 nM CUDC-907 for 24 h. Total RNA was isolated and Bim (C) and Mcl-1 (D) transcripts were determined by real-time reverse transcriptase polymerase chain reaction (RT-PCR). *$P$<0.05, **$P$<0.01, and ***$P$<0.001. (continued on the next page)

obtained in MV4-11 xenograft samples following a single dose of CUDC-907 (Figure 5E). A Mcl-1 protein stability assay using cycloheximide (10 μg/mL) revealed that Mcl-1 levels decreased faster in CUDC-907-treated cells than in vehicle-treated cells, resulting in a significantly shorter half-life (MOLM-13: 58 *vs.* 83 min, *P*=0.0266; U937: 79 *vs.* 94 min, *P*=0.0211) (Figure 5F, G). These results demonstrate that CUDC-907 downregulates Mcl-1 expression by decreasing the stability of Mcl-1 protein.

Phosphorylation of Mcl-1 at T163 has been shown to stabilize Mcl-1 by prolonging its half-life[27] and phosphorylation at S159 enhances ubiquitylation and degradation.[28] In MOLM-13 and U937 cells, CUDC-907 treatment caused downregulation of p-Mcl-1 (T163), while p-Mcl-1 (S159) levels remained unchanged (Figure 5H; upper panel). Treatment with the proteasome inhibitor MG-132, prevented downregulation of Mcl-1 by CUDC-907 (Figure 5H; lower panel). Since ERK has been reported to phosphorylate Mcl-1 at T163[27] and CUDC-907 treatment inactivates ERK, we treated MOLM-13 cells with the ERK inhibitor SCH-772984 and found that treatment did indeed downregulate p-Mcl-1 (T163), while having little to no effect on p-Mcl-1 (S159) levels (*Online Supplementary Figure S6A*). MG-132 treatment prevented downregulation of Mcl-1 following SCH-772984 treatment (*Online Supplementary Figure S6B*). Taken together, these results suggest that CUDC-907 inactivates ERK, resulting in decreased Mcl-1 stability and Mcl-1 protein levels.

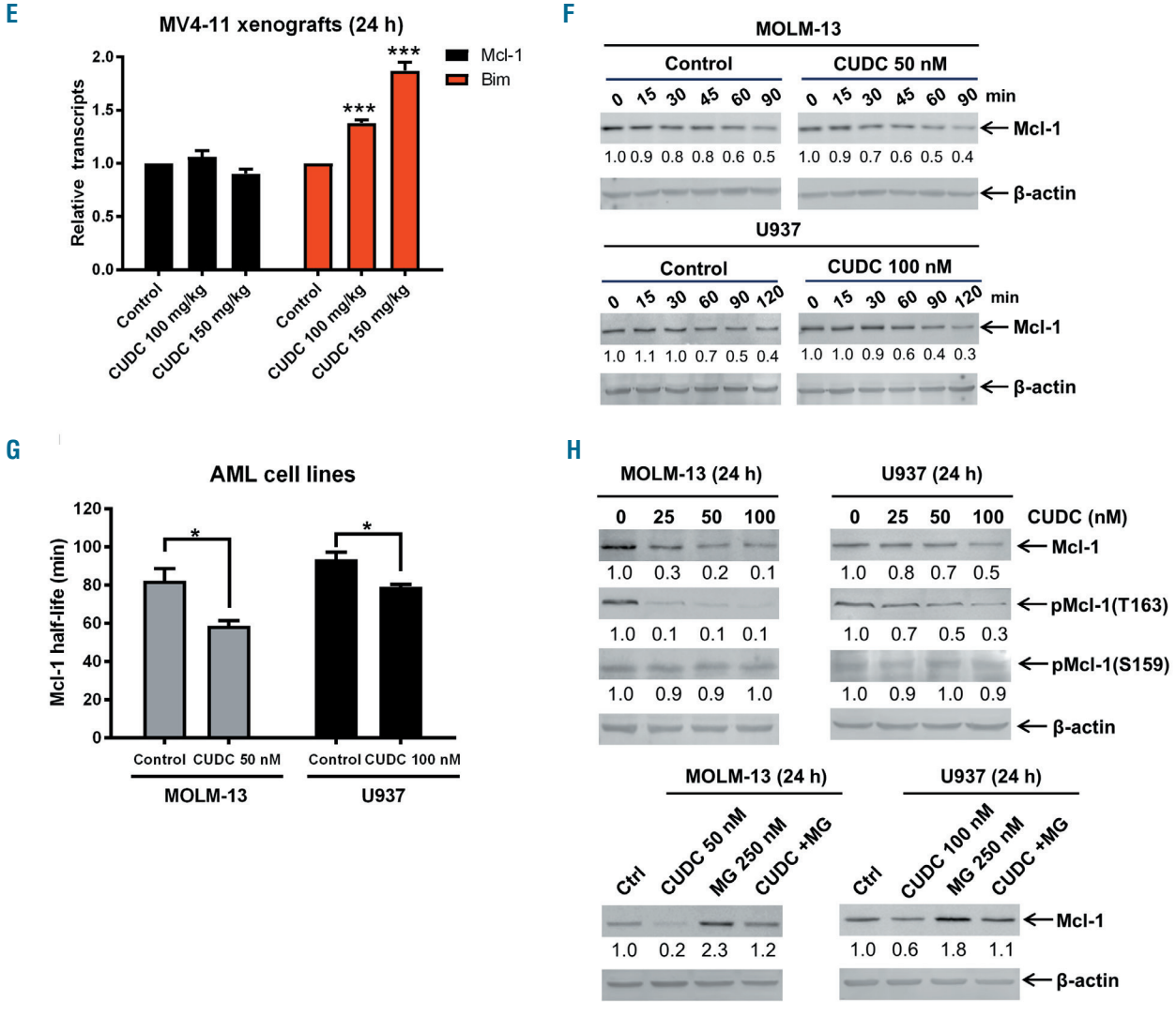


Figure 5. (continued from the previous page) (E) Cells obtained from the MV4-11 xenografts, which were treated with a single dose of CUDC-907, were enriched for human cells. Then total RNA was isolated and real-time RT-PCR performed to determine Mcl-1 and Bim transcripts. ***$P$<0.001. (F, G) MOLM-13 and U937 cells were treated with vehicle control, 50 nM CUDC-907 or 100 nM CUDC-907 for 12 h, washed and then treated with cycloheximide (CHX) for up to 2 h. Whole cell lysates were subjected to western blotting and probed with anti-Mcl-1 or anti-β-actin antibody. The fold changes for the Mcl-1 densitometry measurements, normalized to β-actin and then compared with no drug treatment control, are shown as mean ± standard error of mean. *$P$<0.05. (H) MOLM-13 and U937 cells were treated with CUDC-907, MG-132, or MG-132 plus CUDC-907 for 24 h. Western blot analyses of whole cell lysates are shown. The fold changes for the densitometry measurements, normalized to β-actin and then compared to no drug treatment control, are indicated. RFP: red fluorescent protein; CUDC: CUDC-907; NTC: non-treated control; AML: acute myeloid leukemia; MG: MG-132, a proteasome inhibitor.

### CUDC-907 treatment induces DNA damage in acute myeloid leukemia cells but spares normal human bone marrow mononuclear cells

Western blot analysis revealed that CUDC-907 treatment substantially increased chromatin-bound RPA32 and γH2AX levels, indicating that CUDC-907 treatment induced DNA replication stress and damage (Figure 6A, B). Furthermore, alkaline comet assay results showed that CUDC-907 induced significant increases in DNA strand breaks, as indicated by increased %DNA in the tail (greater %DNA in the tail corresponds to increased DNA strand breaks), for both AML cell lines (Figure 6C, D). The pan-caspase inhibitor Z-VAD-FMK did not have an effect on the %DNA in the tail following CUDC-907 treatment, demonstrating that the increased DNA damage was not a reflection of caspase-dependent cell death (*Online*

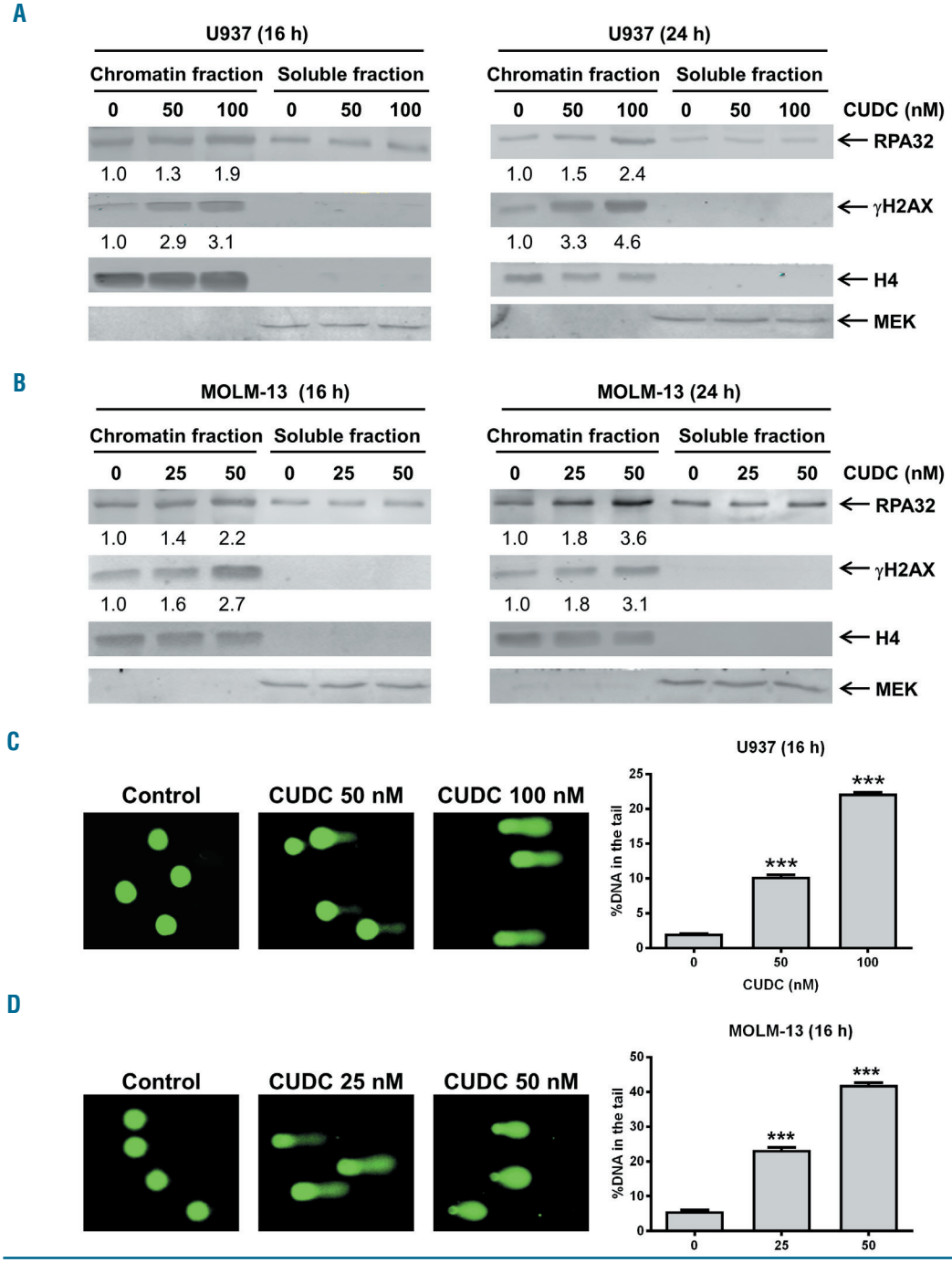


**Figure 6. CUDC-907 treatment induces DNA replication stress and damage in acute myeloid leukemia cells but not in normal human bone marrow mononuclear cells.** (A, B) U937 (A) and MOLM-13 (B) cells were treated with CUDC-907 for 16 or 24 h. Chromatin-bound and soluble RPA32 and γH2AX were analyzed by western blotting and probed with the indicated antibodies. Densitometry measurements, normalized to histone H4 and then compared to the control, are indicated. (C, D) U937 (C) and MOLM-13 (D) cells were treated with CUDC-907 for 16 h and then subjected to alkaline comet assay analysis. Representative images are shown. Data are presented as mean percent DNA in the tail from three replicate gels ± the standard error of mean (SEM). ***$P$<0.001. (continued on the next page)

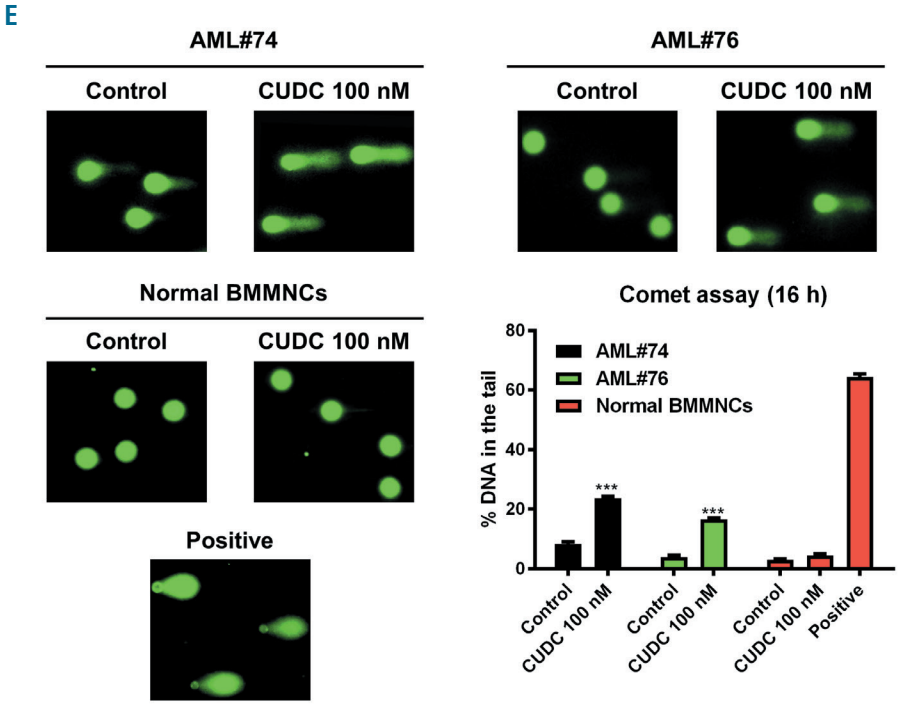


**Figure 6.** (continued from the previous page) (E) Primary cells from patients with acute myeloid leukemia (AML) and normal human bone marrow mononuclear cells (BMMNC) from a single donor were treated with CUDC-907 for 16 h and then subjected to alkaline comet assay analysis. Cells treated with 20 μM daunurubicin (DNR) for 4 h were used as a positive control. Representative images are shown. Data are presented as mean percent DNA in the tail from three replicate gels ± SEM. ***$P$<0.001. (F) U937 cells were treated with CUDC-907 in the presence or absence of LY2603618 (LY), MK-1775 (MK), or hydroxyurea (HU) for 24 h and then subjected to annexin V/propidium iodide (PI) staining and flow cytometry analyses. ***$P$<0.001. (G-I) MV4-11, U937 and MOLM-13 AML cell lines and two primary AML patients samples were treated with 0-100 nM CUDC-907 for 24 h. Total RNA was isolated and CHK1 (G), RRM1 (H), and Wee1 (I) transcripts were determined by real-time reverse transcriptase polymerase chain reaction (RT-PCR). *$P$<0.05, **$P$<0.01, and ***P<0.001. (J) Cells obtained from the MV4-11 xenografts, which were treated with a single dose of CUDC-907, were enriched for human cells. Then total RNA was isolated and real-time RT-PCR performed to determine CHK1, RRM1, and Wee1 transcripts. *$P$<0.05, **$P$<0.01, and ***$P$<0.001.

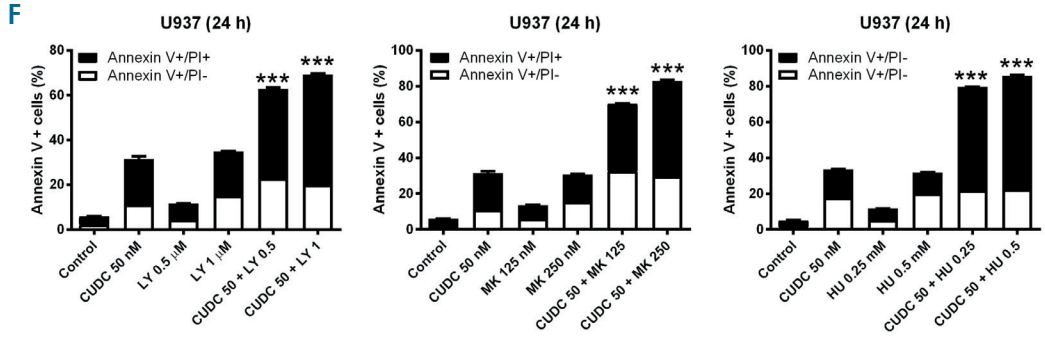


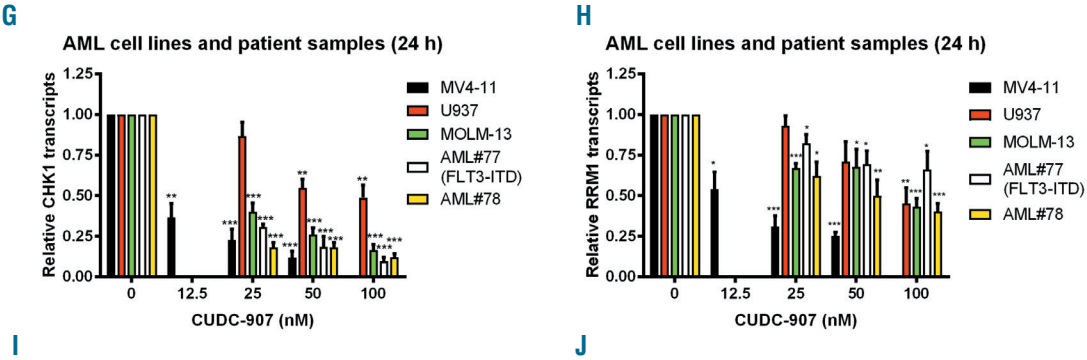


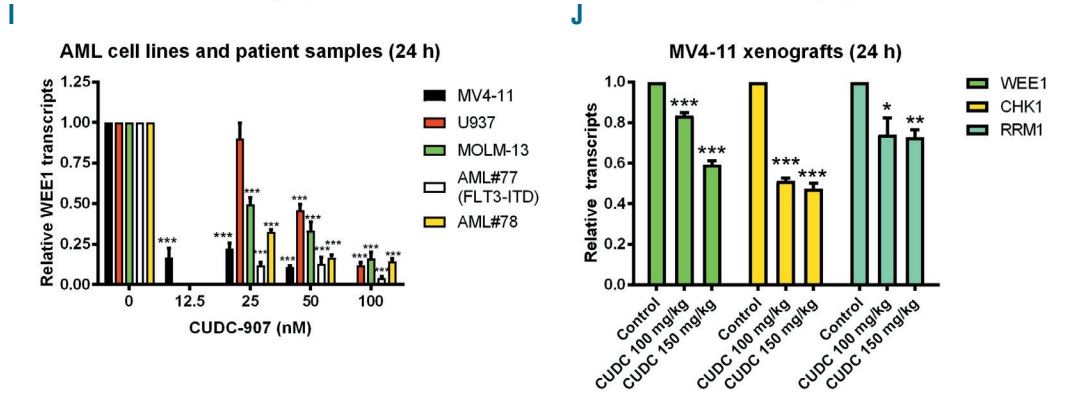

*Supplementary Figure S7*). DNA strand breaks induced by CUDC-907 were also detected in two primary AML patient samples but not in normal human bone marrow mononuclear cells (Figure 6E), suggesting that CUDC-907 does not induce DNA damage in normal hematopoietic cells. To determine the functional role of CHK1, Wee1, and RRM1 in apoptosis induced by CUDC-907, U937 cells were treated with CUDC-907 alone or in combination with the CHK1 inhibitor LY2603618, Wee1 inhibitor MK-1775, or the RR inhibitor hydroxyurea for 24 h. Annexin V/PI staining and flow cytometry revealed that each inhibitor significantly enhanced CUDC-907-induced apoptosis (Figure 6F), which suggests that CHK1, Wee1, and RRM1 also play important roles in CUDC-907-induced apoptosis in the cells. Real-time reverse transcriptase PCR results showed that CUDC-907 treatment caused significant decreases of CHK1, Wee1, and RRM1 transcripts in the AML cells both *in vitro* and *in vivo* (Figure 6G-J), suggesting that CUDC-907 downregulates CHK1, Wee1, and RRM1 expression in the cells through transcriptional regulation. While it has been reported that non-isoform selective PI3K inhibitors also inhibit DNA-PK, inhibition of DNA-PK is not likely to have contributed to the increased DNA damage-induced by CUDC-907 since its effect on DNA-PK activity was minimal (*Online Supplementary Figure S8*).

## CUDC-907 downregulates c-Myc in acute myeloid leukemia cells

CUDC-907 treatment was shown to downregulate c-Myc protein in diffuse large B-cell lymphoma cells.[16] Since c-Myc is an oncoprotein that is frequently activated in AML cells and plays a role in leukemogenesis,[29,30] we next determined the role of c-Myc in CUDC-907-induced apoptosis in AML cells. Indeed, CUDC-907 treatment decreased expression of c-Myc in AML cell lines and a primary AML sample (Figure 7A). In addition, decreased expression was detected in our MV4-11 xenograft mouse model following a single dose of CUDC-907 (Figure 7B). The pan-caspase inhibitor Z-VAD-FMK did not have an effect on downregulation of c-Myc by CUDC-907 (*Online Supplementary Figure S9A*). Furthermore, treatment with SAHA, GDC-0941, and SAHA plus GDC-0941 did not reduce c-Myc protein levels, again suggesting that the hybrid is more potent than the parental compounds (*Online Supplementary Figure S9B*). In both MOLM-13 and U937 cells, downregulation of c-Myc was detected as early as 4 h after CUDC-907 treatment (Figure 7C). c-Myc transcript levels were decreased in AML cell lines, two primary AML patient samples (Figure 7D) and in the MV4-11 xenograft mouse model following a single dose of CUDC-907 (Figure 7E). Overexpression of c-Myc resulted in partial inhibition of CUDC-907-induced apoptosis (Figure

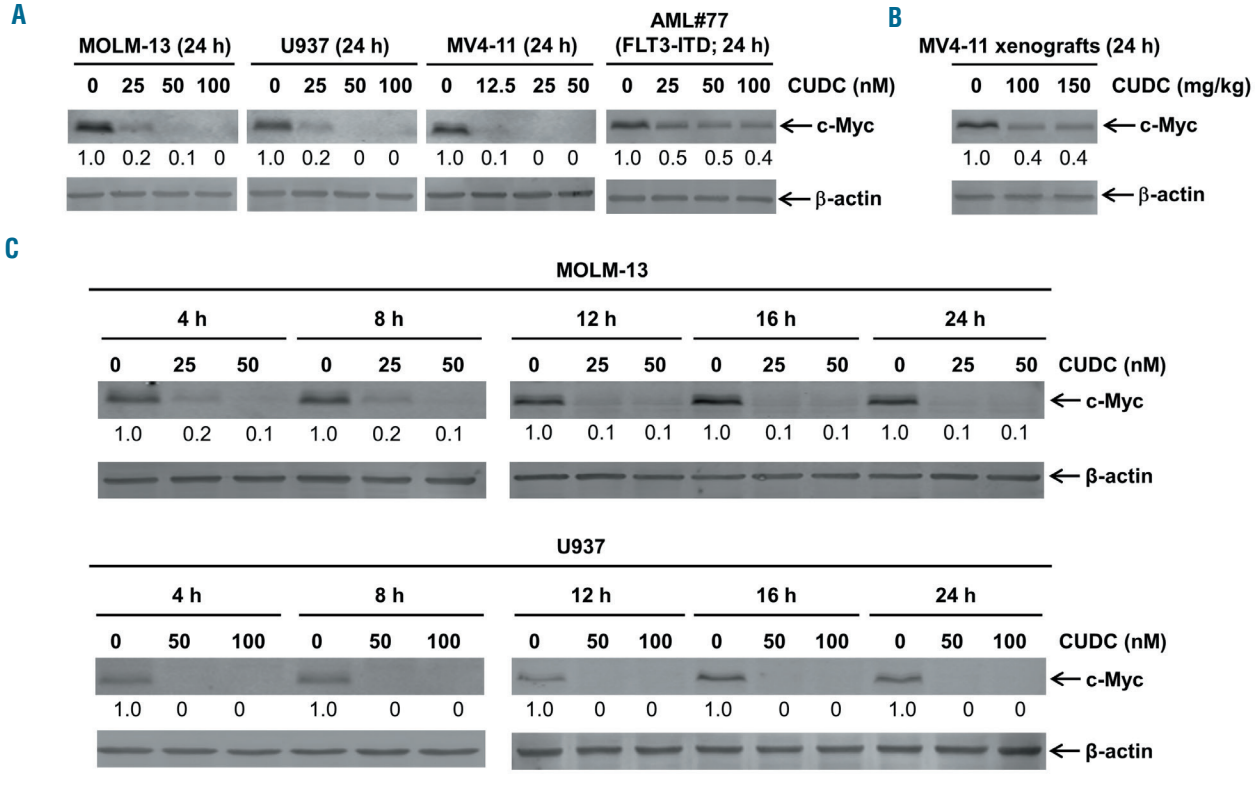


**Figure 7. CUDC-907 treatment downregulates c-Myc in acute myeloid leukemia cells.** (A) Acute myeloid leukemia (AML) cell lines and primary AML patient sample AML#77 were treated with CUDC-907 for 24 h. Whole cell lysates were subjected to western blotting. Normalized densitometry measurements are shown. (B) the MV4-11 xenograft model was treated with a single dose of CUDC-907 21 days after cell injection. Bone marrow cells were harvested 24 h after treatment. Human cells were enriched and then whole cell lysates were subjected to western blotting. (C) MOLM-13 and U937 cells were treated with CUDC-907 for up to 24 h. Whole cell lysates were subjected to western blotting. (continued on the next page)

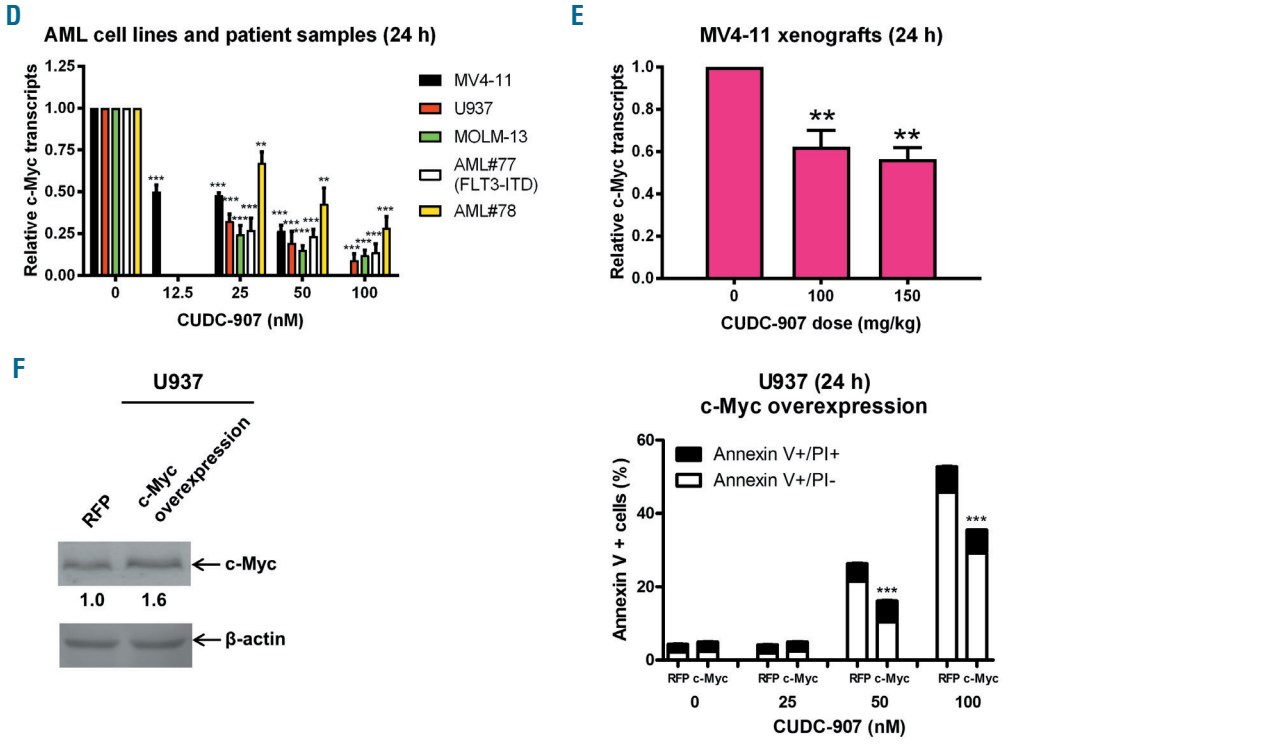


**Figure 7.** (continued from the previous page) (D) MV4-11, U937 and MOLM-13 AML cell lines and two primary AML patient samples were treated with 0-100 nM CUDC-907 for 24 h. Total RNA was isolated and c-Myc transcripts were determined by real-time reverse transcriptase polymerase chain reaction (RT-PCR). ***P*<0.01, ****P*<0.001. (E) Cells obtained from the MV4-11 xenografts, which were treated with a single dose of CUDC-907, were enriched for human cells. Then total RNA was isolated and real-time RT-PCR performed to determine c-Myc transcripts. ***P*<0.01. (F) U937 cells were infected with Precision LentiORF c-Myc and red fluorescent protein (RFP) control lentivirus particles overnight, then washed and incubated for 24 h. The whole cell lysate from one aliquot of the cells was subjected to western blotting. The fold changes for the c-Myc densitometry measurements, normalized to β-actin and then compared to non-treated control (NTC), are indicated (left panel). The other aliquot of the cells was treated with CUDC-907 for 24 h and then subjected to annexin V/propidium iodide (PI) staining and flow cytometry analysis. ****P*<0.001 (right panel). (G) Proposed mechanism of action of CUDC-907 treatment: (i) CUDC-907 inactivates ERK and inhibits PI3K resulting in reduced Mcl-1 expression; (ii) CUDC-907 inhibits histone deacetylases (HDAC) which downregulates CHK1, Wee1, and/or RRM1, reducing DNA repair; (iii) CUDC-907 inhibits HDAC decreasing c-Myc; and (iv) CUDC-907 inhibits HDAC which upregulates Bim. The foregoing molecular changes lead to apoptosis.

7F), demonstrating that c-Myc plays a role in CUDC-907-induced apoptosis in AML cells.

## Discussion

A major hurdle in the successful treatment of AML is resistance to standard therapies, which warrants the development of novel strategies. Here, we showed that CUDC-907 has promising antileukemic activity against AML cell lines, both *in vitro* and *in vivo*, and against leukemia progenitor cells from primary AML patient samples. CUDC-907 treatment decreased expression of the anti-apoptotic protein Mcl-1 and increased expression of the pro-apoptotic protein Bim. Ectopic overexpression of Mcl-1 and shRNA knockdown of Bim demonstrated that both proteins play important roles in CUDC-907-induced apoptosis in AML cells (Figure 5A, B). Our results are consistent with the known effects of PI3K and HDAC inhibition, which have been shown to decrease the anti-apoptotic protein Mcl-1 and upregulate the pro-apoptotic protein Bim.[22-25] In addition, they are in agreement with the findings of Rahmani *et al.* who demonstrated that Bim and Mcl-1 play a role in HDAC and PI3K inhibitor lethality in non-Hodgkin lymphoma.[12] Our data show that CUDC-907 treatment decreases the stability of Mcl-1, at least partially through its ability to inactivate ERK (Figure 5D-H). Based on the reported transcriptional regulation of Bim following HDAC inhibitor treatment[31,32] and the increase in Bim transcripts following CUDC-907 treatment (Figure

5C), the upregulation of Bim (Figure 3B) was likely due to transcriptional regulation mediated by the HDAC inhibitor moiety of CUDC-907. However, given the evidence that the ERK pathway regulates Bim degradation,[33,34] post-transcriptional mechanisms cannot be ruled out. Additionally, inactivation of AKT and ERK may also contribute to the antileukemic activity of CUDC-907 through other downstream targets.[12,14]

HDAC inhibitors have been shown to induce differentiation, cell cycle arrest, DNA damage, and apoptosis in AML cells.[20,26,35-37] One mechanism through which HDAC inhibitors exert their anticancer activity is through downregulation of DNA damage response proteins, such as CHK1 and Wee1, as we and others have reported.[23-26] In agreement, we detected downregulation of CHK1 and Wee1 protein and transcript levels (Figures 3C and 6G, I, and J). HDAC inhibitor-induced downregulation of CHK1 and Wee1 has been shown to be mediated through downregulation of E2F1.[37,38] However, the decrease of E2F1 was not consistent in the AML cell lines and primary AML patient sample. CUDC-907 treatment caused decreases of E2F1, CHK1, and Wee1 in three AML cell lines and one primary AML patient's sample. However, in the other primary AML patient sample, CUDC-907 treatment did not result in a decrease of E2F1 protein but did decrease both CHK1 and Wee1 protein levels. These results suggest that downregulation of CHK1 and Wee1 was probably mediated through transcript regulation, though it may not have been entirely mediated through downregulation of E2F1.

CUDC-907 treatment also decreased RRM1 protein and transcript levels (Figures 3C and 6H, J), suggesting that downregulation of this gene was probably mediated by a transcriptional mechanism. Based on our results using hydroxyurea, RRM1 likely played an important role in CUDC-907-induced DNA damage. Inhibition of RR decreases dNTP pools, resulting in DNA replication fork stalling, impaired DNA repair, and DNA damage.[39] In agreement with Sun *et al.*,[16] we found that CUDC-907 treatment reduced expression of c-Myc protein prior to induction of apoptosis (Figures 4C, D and 7C). Given its role in cell growth, proliferation, and survival, the early downregulation of c-Myc may play a more prominent role in CUDC-907-induced apoptosis since changes in CHK1, Wee1, RRM1, Bim, and Mcl-1 levels occur after c-Myc downregulation.

*FLT3*-ITD AML has been shown to be associated with increased DNA damage and misrepair,[40] potentially making such leukemias more sensitive to DNA replication fork stalling, impaired DNA repair, and DNA damage. Interestingly, we found that primary AML samples from patients with *FLT3*-ITD were significantly more sensitive to CUDC-907 *ex vivo* (Figure 2A). *FLT3*-ITD has also been shown to constitutively activate downstream PI3K and ERK pathways, conferring resistance to PI3K and ERK inhibitors. However, HDAC inhibitors have been shown to upregulate ubiquitin conjugase[41] and inhibit HSP90 resulting in proteasomal degradation of FLT3.[42,43] Consistent with those reports, CUDC-907 treatment did indeed decrease FLT3 protein levels in the *FLT3*-ITD AML cell line MOLM-13 (*Online Supplementary Figure S10*). Thus, the HDAC inhibitor moiety of CUDC-907 reduces FLT3 levels, relieving constitutive activation of the PI3K and ERK pathways, and allowing the PI3K inhibitor function of CUDC-907 to induce AML cell death. This may explain the superior response of *FLT3*-ITD AML cells to CUDC-907 (Figure 2A), although the effects of CUDC-907 on AML cell apoptosis, colony-formation capacity, and FLT3 protein levels need to be further elucidated in additional primary samples from patients with *FLT3*-ITD AML.

Results of the first phase I trial of CUDC-907 were recently published, outlining the safety, tolerability, and preliminary activity in patients with lymphoma or multiple myeloma.[17] In that study, the recommended dosing for further clinical studies was identified to be 60 mg administered orally, once daily for 5 days, followed by 2 days off treatment, as there were no dose-limiting toxicities at this dosing and schedule. In addition, side effects were consistent with the known profile of HDAC or PI3K inhibitors and deemed manageable. Our data show promising *in vivo* efficacy against an AML cell line-derived xenograft mouse model, supporting further clinical development of CUDC-907 as an AML-focused therapy. While modest weight loss was seen after CUDC-907 treatment (nadir: -5.4% on day 22, 2 days after last treatment), it was completely reversible within 4 days. This fact coupled with the observed modest survival benefit produced from the interrupted treatment schedule indicate that either or both the dosing and schedule can be further optimized (i.e. in hindsight, the drug was so well tolerated that the 4-day interruption of treatment may not have been necessary). Furthermore, the tolerability of CUDC-907 suggests that it may be used in combination with other therapies. Conventional chemotherapy drugs, such as cytarabine or daunorubicin, may synergize with CUDC-907 as these drugs induce DNA damage and would likely add further insult to the stressed DNA repair system following CUDC-907 treatment.

In summary, our study demonstrates that CUDC-907 induces DNA damage and apoptosis in AML cell lines and primary patients' samples, and targets AML progenitor cells while sparing normal hematopoietic cells *in vitro*. In addition, our initial *in vivo* study generated a promising increase in survival following CUDC-907 monotherapy. As a dual inhibitor, CUDC-907 lends itself to the possibility of combination therapies to further eliminate AML and prevent disease relapse. Our findings provide new insights into the mechanism of action of CUDC-907 in AML cells (Figure 7G) and support its clinical development for the treatment of AML.

***Acknowledgments***

*This study was supported by Jilin University, Changchun, China, the Barbara Ann Karmanos Cancer Institute, Wayne State University School of Medicine, and by grants from the National Natural Science Foundation of China, NSFC 31671438 and NSFC 31471295, Hyundai Hope on Wheels, LaFontaine Family/U Can-Cer Vive Foundation, Kids Without Cancer, Children's Hospital of Michigan Foundation, Decerchio/Guisewite Family, Justin's Gift, Elana Fund, Ginopolis/Karmanos Endowment and the Ring Screw Textron Endowed Chair for Pediatric Cancer Research. The Animal Models and Therapeutics Evaluation Core is supported, in part, by NIH Center grant P30 CA022453 to the Karmanos Cancer Institute at Wayne State University. The funders had no role in study design, data collection, analysis and interpretation of data, decision to publish, or preparation of the manuscript.*

## References


1. Marcucci G, Haferlach T, Dohner H. Molecular genetics of adult acute myeloid leukemia: prognostic and therapeutic implications. J Clin Oncol. 2011;29(5):475-486.
2. Rubnitz JE, Inaba H, Dahl G, et al. Minimal residual disease-directed therapy for childhood acute myeloid leukaemia: results of the AML02 multicentre trial. Lancet Oncol. 2010;11(6):543-552.
3. Doan PL, Chute JP. The vascular niche: home for normal and malignant hematopoietic stem cells. Leukemia. 2012;26(1):54-62.
4. Min YH, Eom JI, Cheong JW, et al. Constitutive phosphorylation of Akt/PKB protein in acute myeloid leukemia: its significance as a prognostic variable. Leukemia. 2003;17(5):995-997.
5. Gallay N, Dos Santos C, Cuzin L, et al. The level of AKT phosphorylation on threonine 308 but not on serine 473 is associated with high-risk cytogenetics and predicts poor overall survival in acute myeloid leukaemia. Leukemia. 2009;23(6):1029-1038.
6. Guo W, Schubbert S, Chen JY, et al. Suppression of leukemia development caused by PTEN loss. Proc Natl Acad Sci U S A. 2011;108(4):1409-1414.
7. Xu Q, Simpson SE, Scialla TJ, Bagg A, Carroll M. Survival of acute myeloid leukemia cells requires PI3 kinase activation. Blood. 2003;102(3):972-980.
8. Fransecky L, Mochmann LH, Baldus CD. Outlook on PI3K/AKT/mTOR inhibition in acute leukemia. Mol Cell Ther. 2015;3:2.
9. Rozengurt E, Soares HP, Sinnet-Smith J. Suppression of feedback loops mediated by PI3K/mTOR induces multiple overactivation of compensatory pathways: an unintended consequence leading to drug resistance. Mol Cancer Ther. 2014;13(11):2477-2488.
10. Mendoza MC, Er EE, Blenis J. The Ras-ERK and PI3K-mTOR pathways: cross-talk and compensation. Trends Biochem Sci. 2011;36(6):320-328.
11. Rahmani M, Yu C, Reese E, et al. Inhibition of PI-3 kinase sensitizes human leukemic cells to histone deacetylase inhibitor-mediated apoptosis through p44/42 MAP kinase inactivation and abrogation of p21(CIP1/WAF1) induction rather than AKT inhibition. Oncogene. 2003;22(40):6231-6242.
12. Rahmani M, Aust MM, Benson EC, Wallace L, Friedberg J, Grant S. PI3K/mTOR inhibition markedly potentiates HDAC inhibitor activity in NHL cells through BIM- and MCL-1-dependent mechanisms in vitro and in vivo. Clin Cancer Res. 2014;20(18):4849-4860.
13. Gupta M, Ansell SM, Novak AJ, Kumar S, Kaufmann SH, Witzig TE. Inhibition of histone deacetylase overcomes rapamycin-mediated resistance in diffuse large B-cell lymphoma by inhibiting Akt signaling through mTORC2. Blood. 2009;114(14):2926-2935.
14. Qian C, Lai CJ, Bao R, et al. Cancer network disruption by a single molecule inhibitor targeting both histone deacetylase activity and phosphatidylinositol 3-kinase signaling. Clin Cancer Res. 2012;18(15):4104-4113.
15. Kotian S, Zhang L, Boufraqech M, et al. Dual Inhibition of HDAC and tyrosine kinase signaling pathways with CUDC-907 inhibits thyroid cancer growth and metastases. Clin Cancer Res. 2017;23(17): 5044-5054.
16. Sun K, Atoyan R, Borek MA, et al. Dual HDAC and PI3K inhibitor CUDC-907 Downregulates MYC and suppresses growth of MYC-dependent cancers. Mol Cancer Ther. 2017;16(2):285-299.
17. Younes A, Berdeja JG, Patel MR, et al. Safety, tolerability, and preliminary activity of CUDC-907, a first-in-class, oral, dual inhibitor of HDAC and PI3K, in patients with relapsed or refractory lymphoma or multiple myeloma: an open-label, dose-escalation, phase 1 trial. Lancet Oncol. 2016;17(5):622-631.
18. Niu X, Wang G, Wang Y, et al. Acute myeloid leukemia cells harboring MLL fusion genes or with the acute promyelocytic leukemia phenotype are sensitive to the Bcl-2-selective inhibitor ABT-199. Leukemia. 2014;28(7):1557-1560.
19. Ma J, Li X, Su Y, et al. Mechanisms responsible for the synergistic antileukemic interactions between ATR inhibition and cytarabine in acute myeloid leukemia cells. Sci Rep. 2017;7:41950.
20. Xie C, Edwards H, Xu X, et al. Mechanisms of synergistic antileukemic interactions between valproic acid and cytarabine in pediatric acute myeloid leukemia. Clin Cancer Res. 2010;16(22):5499-5510.
21. Edwards H, Xie C, LaFiura KM, et al. RUNX1 regulates phosphoinositide 3-kinase/AKT pathway: role in chemotherapy sensitivity in acute megakaryocytic leukemia. Blood. 2009;114(13):2744-2752.
22. Martelli AM, Evangelisti C, Chappell W, et al. Targeting the translational apparatus to improve leukemia therapy: roles of the PI3K/PTEN/Akt/mTOR pathway. Leukemia. 2011;25(7):1064-1079.
23. Inoue S, Riley J, Gant TW, Dyer MJ, Cohen GM. Apoptosis induced by histone deacetylase inhibitors in leukemic cells is mediated by Bim and Noxa. Leukemia. 2007;21(8): 1773-1782.
24. Chen S, Dai Y, Pei XY, Grant S. Bim upregulation by histone deacetylase inhibitors mediates interactions with the Bcl-2 antagonist ABT-737: evidence for distinct roles for Bcl-2, Bcl-xL, and Mcl-1. Mol Cell Biol. 2009;29(23):6149-6169.
25. Fiskus W, Sharma S, Saha S, et al. Pre-clinical efficacy of combined therapy with novel beta-catenin antagonist BC2059 and histone deacetylase inhibitor against AML cells. Leukemia. 2015;29(6):1267-1278.
26. Qi W, Zhang W, Edwards H, et al. Synergistic anti-leukemic interactions between panobinostat and MK-1775 in acute myeloid leukemia ex vivo. Cancer Biol Ther. 2015;16(12):1784-1793.
27. Domina AM, Vrana JA, Gregory MA, Hann SR, Craig RW. MCL1 is phosphorylated in the PEST region and stabilized upon ERK activation in viable cells, and at additional sites with cytotoxic okadaic acid or taxol. Oncogene. 2004;23(31):5301-5315.
28. Maurer U, Charvet C, Wagman AS, Dejardin E, Green DR. Glycogen synthase kinase-3 regulates mitochondrial outer membrane permeabilization and apoptosis by destabilization of MCL-1. Mol Cell. 2006;21(6):749-760.
29. Hoffman B, Amanullah A, Shafarenko M, Liebermann DA. The proto-oncogene c-myc in hematopoietic development and leukemogenesis. Oncogene. 2002;21(21):3414-3421.
30. Renneville A, Roumier C, Biggio V, et al. Cooperating gene mutations in acute myeloid leukemia: a review of the literature. Leukemia. 2008;22(5):915-931.
31. Xargay-Torrent S, Lopez-Guerra M, Saborit-Villarroya I, et al. Vorinostat-induced apoptosis in mantle cell lymphoma is mediated by acetylation of proapoptotic BH3-only gene promoters. Clin Cancer Res. 2011;17(12):3956-3968.
32. Yang Y, Zhao Y, Liao W, et al. Acetylation of FoxO1 activates Bim expression to induce apoptosis in response to histone deacetylase inhibitor depsipeptide treatment. Neoplasia. 2009;11(4):313-324.
33. Ley R, Balmanno K, Hadfield K, Weston C, Cook SJ. Activation of the ERK1/2 signaling pathway promotes phosphorylation and proteasome-dependent degradation of the BH3-only protein, Bim. J Biol Chem. 2003;278(21):18811-18816.
34. Luciano F, Jacquel A, Colosetti P, et al. Phosphorylation of Bim-EL by Erk1/2 on serine 69 promotes its degradation via the proteasome pathway and regulates its proapoptotic function. Oncogene. 2003;22(43):6785-6793.
35. Quintas-Cardama A, Santos FP, Garcia-Manero G. Histone deacetylase inhibitors for the treatment of myelodysplastic syndrome and acute myeloid leukemia. Leukemia. 2011;25(2):226-235.
36. Minucci S, Pelicci PG. Histone deacetylase inhibitors and the promise of epigenetic (and more) treatments for cancer. Nat Rev Cancer. 2006;6(1):38-51.
37. Xie C, Drenberg C, Edwards H, et al. Panobinostat enhances cytarabine and daunorubicin sensitivities in AML cells through suppressing the expression of BRCA1, CHK1, and Rad51. PLoS One. 2013;8(11):e79106.
38. Carrassa L, Broggini M, Vikhanskaya F, Damia G. Characterization of the 5' flanking region of the human Chk1 gene: identification of E2F1 functional sites. Cell Cycle. 2003;2(6):604-609.
39. Aye Y, Li M, Long MJ, Weiss RS. Ribonucleotide reductase and cancer: biological mechanisms and targeted therapies. Oncogene. 2015;34(16):2011-2021.
40. Sallmyr A, Fan J, Datta K, et al. Internal tandem duplication of FLT3 (FLT3/ITD) induces increased ROS production, DNA damage, and misrepair: implications for poor prognosis in AML. Blood. 2008;111(6):3173-3182.
41. Buchwald M, Pietschmann K, Muller JP, Bohmer FD, Heinzel T, Kramer OH. Ubiquitin conjugase UBCH8 targets active FMS-like tyrosine kinase 3 for proteasomal degradation. Leukemia. 2010;24(8):1412-1421.
42. Bali P, George P, Cohen P, et al. Superior activity of the combination of histone deacetylase inhibitor LAQ824 and the FLT-3 kinase inhibitor PKC412 against human acute myelogenous leukemia cells with mutant FLT-3. Clin Cancer Res. 2004;10(15):4991-4997.
43. Nishioka C, Ikezoe T, Yang J, Takeuchi S, Koeffler HP, Yokoyama A. MS-275, a novel histone deacetylase inhibitor with selectivity against HDAC1, induces degradation of FLT3 via inhibition of chaperone function of heat shock protein 90 in AML cells. Leuk Res. 2008;32(9):1382-1392.